ALIEN EARTHS

Which Nearby Planetary Systems Are Likely to Host Habitable Planets and Life?

MONTHLY NEWSLETTER

February 2026

Alien Earths is part of NASA's Nexus for Exoplanetary System Science program, which carries out coordinated research toward the goal of searching for and determining the frequency of habitable extrasolar planets with atmospheric biosignatures in the Solar neighborhood.

Our interdisciplinary teams include astrophysicists, planetary scientists, cosmochemists, material scientists, chemists, biologists, and physicists.

The Principal Investigator of Alien Earths is Daniel Apai (University of Arizona). The projects' lead institutions are The University of Arizona's Steward Observatory and Lunar and Planetary Laboratory.

For a complete list of publications, please visit the **AE Library** on the SAO/NASA Astrophysics Data System.

Recent Publications

Why Estimating $\eta_\oplus$ is Difficult: A Kepler Centric Perspective

.....

JWST TRAPPIST-1 e/b Program: Motivation and First Observations

.....

Modeling the Impact of Unresolved Stellar Companions on Detection Sensitivity in Kepler's Small-planet Occurrence Rates

.....

A Thick Volatile Atmosphere on the Ultrahot Super-Earth TOI-561 b

.....

Dust Recycling and Icy Volatile Enhancement (DRIVE): A Novel Method of Volatile Enrichment in Cold Giant Planets

.....

The formation and structure of iron-dominated planetesimals

.....

Detection and characterization of a 106-day transiting Jupiter: TOI-2449 b/NGTS-36b

.....

HWO Target Stars and Systems: A Prioritized Community List of Potential Stellar Targets for Habitable Worlds Observatory's ExoEarth Survey

.....

Radius valley scaling among low-mass stars with TESS

.....

Why Estimating $\eta_\oplus$ is Difficult: A Kepler Centric Perspective

Steve Bryson, Michelle Kunimoto, Ruslan Belikov, Galen J. Bergsten, Sakhee Bhure, William J. Borucki, Douglas A. Caldwell, Aritra Chakrabarty, Rachel B. Fernandes, Matthias Y. He, Jon M. Jenkins, Kristo Ment, Michael R. Meyer, Gijs D. Mulders, Ilaria Pascucci, and Peter Plavchan

Publications of the Astronomical Society of the Pacific, Volume 137, Number 12

$\eta_\oplus$, the occurrence rate of rocky habitable zone exoplanets orbiting Sun-like stars, is of great interest to both the astronomical community and the general public. The Kepler space telescope has made it possible to estimate $\eta_\oplus$, but estimates by different groups vary by more than an order of magnitude. We identify several causes for this range of estimates. We first review why, despite being designed to estimate $\eta_\oplus$, Kepler's observations are not sufficient for a high-confidence estimate, due to Kepler's detection limit coinciding with the $\eta_\oplus$ regime. This results in a need to infer $\eta_\oplus$, for example extrapolating from a regime of non-habitable zone, non-rocky exoplanets. We examine two broad classes of causes that can account for the large discrepancy in $\eta_\oplus$ found in the literature: (a) differences in definitions and input data between studies, and (b) fundamental limits in Kepler data that lead to large uncertainties and poor accuracy. We highlight the risk of large biases when using extrapolation to describe small exoplanet populations in the habitable zone. We discuss how $\eta_\oplus$ estimates based on Kepler data can be improved, such as reprocessing Kepler data for more complete, higher-reliability detections and better exoplanet catalog characterization. We briefly survey upcoming space telescopes capable of measuring $\eta_\oplus$, and how they can be used to supplement Kepler data.

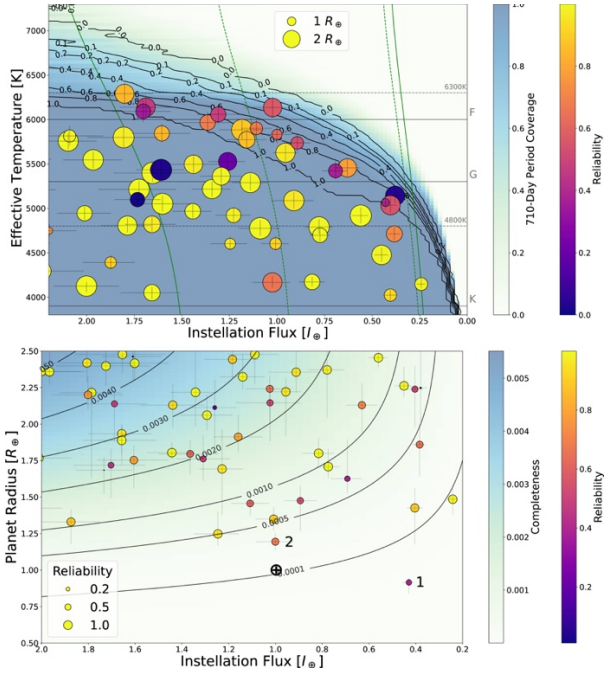

Two views of the DR25 PC population around FGK stars with radii smaller than 2.5 $R_\oplus$ and instellation flux near their host star's habitable zone around main sequence dwarf stars. Top: instellation flux versus stellar effective temperature, showing the habitable zone and Kepler observational coverage. The background color map gives, at each point, the fraction of Kepler target stars at that effective temperature whose exoplanets at that instellation flux would have orbital periods of 710 days or less, so it is possible to observe three transits. The contours show the fraction of exoplanets with periods of 500 days or less, indicating available completeness measurements. The solid green lines are the boundaries of the optimistic habitable zone, while the dashed green lines are the boundaries of the conservative habitable zone. The exoplanets are sized by their radius and colored by their catalog reliability. Bottom: Instellation flux versus exoplanet radius. The color map and contours show the average completeness for the stellar population (in the case of zero-completeness extrapolation, see Section 4.1.3). The exoplanets are sized and colored by catalog reliability, with radius and instellation flux error bars. In the lower panel the ⊕ symbol shows the Earth. The two numbered exoplanets are discussed in Section 4.2.2. Reproduced from Bryson et al. (2021). The Author(s). CC BY 4.0. Reliability values in both panels are from Bryson et al. (2020a).

JWST TRAPPIST-1 e/b Program: Motivation and First Observations

Natalie H. Allen, Néstor Espinoza, V. A. Boehm, Caleb I. Cañas, Kevin B. Stevenson, Nikole K. Lewis, Ryan J. MacDonald, Brett M. Morris, Eric Agol, Knicole Colón, Hannah Diamond-Lowe, Ana Glidden, Amélie Gressier, Jingcheng Huang, Zifan Lin, Douglas Long, Dana R. Louie, Meredith A. MacGregor, Laurent Pueyo, Benjamin V. Rackham, Sukrit Ranjan, Sara Seager, Guadalupe Tovar Mendoza, Jeff A. Valenti, Daniel Valentine, Roeland P. van der Marel, and Hannah R. Wakeford

The Astronomical Journal, Volume 171, Number 2

One of the forefront goals in the field of exoplanets is the detection of an atmosphere on a temperate terrestrial exoplanet, and among the best suited systems to do so is TRAPPIST-1. However, JWST transit observations of the TRAPPIST-1 planets show significant contamination from stellar surface features that we are unable to confidently model. Here, we present the motivation and first observations of our JWST multicycle program of TRAPPIST-1 e, which utilize close transits of the airless TRAPPIST-1 b to model-independently correct for stellar contamination, with the goal of determining whether TRAPPIST-1 e has an Earth-like mean molecular weight atmosphere containing CO_2. We present our simulations, which show that with 15 close transit observations, we will be able to detect this atmosphere on TRAPPIST-1 e at $\Delta \ln Z = 5$ or greater confidence assuming we are able to correct for stellar contamination using the close transit observations. We also show the first three observations of our program. We find that our ability to correct for stellar contamination can be inhibited when strong stellar flares are present, as flares can break the assumption that the star does not change meaningfully between planetary transits. The cleanest observation demonstrates the removal of stellar contamination contribution through an increased preference for a flat line over the original TRAPPIST-1 e spectrum, but highlights how minor data analysis assumptions can propagate significantly when searching for small atmospheric signals. This is amplified when using the signals from multiple planets, which is important to consider as we continue our atmospheric search.

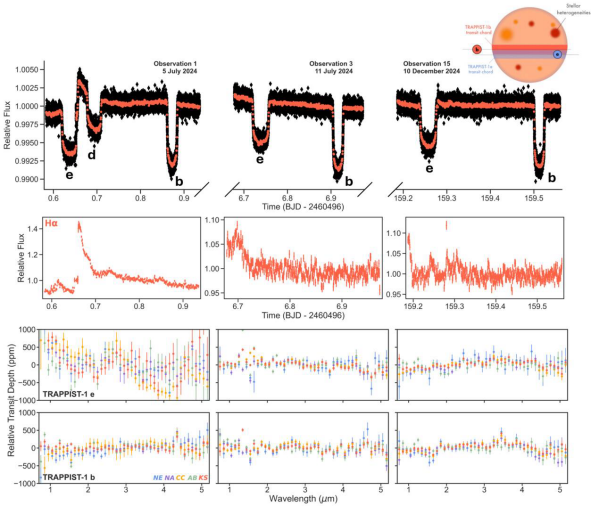

Top: white light curves of observation 1, observation 3, and observation 15 from the N.A. reduction, both at native time resolution in black and binned to 25× in red for visibility. All transits are labeled by planet. Observation 1 also has a large flare that occurs right before the egress of planet e. Shown in the upper right is a schematic of our proposed setup, with the true overlapping planetary transit chords taken from E. Agol et al. (2021). Middle: Hα light curve from the N.A. reduction. Peaks in Hα correspond to flaring events, many of which are not visible in the white light curve, at least without hints to their location from the Hα signature. Note that the light curves are binned in time to 50× (to approximately 70 s bins) relative to that shown in the white light curve for visibility in the low signal single wavelengths shown. Bottom: transmission spectrum of TRAPPIST-1 e (top) and TRAPPIST-1 b (bottom) for observation 1, observation 3, and observation 15 from left to right.

Modeling the Impact of Unresolved Stellar Companions on Detection Sensitivity in Kepler's Small-planet Occurrence Rates

Galen J. Bergsten, David R. Ciardi, Jessie L. Christiansen, Catherine A. Clark, Ilaria Pascucci, Courtney D. Dressing, Kevin K. Hardegree-Ullman, and Michael B. Lund

The Astronomical Journal, Volume 171, Number 2

Unresolved stellar companions can cause both underestimations in the radii of transiting planets and overestimations of their detectability, affecting our ability to reliably measure planet occurrence rates. To quantify the latter, we identified a control sample of 198 Kepler stars with sensitivity to Earth-like planets if they were single stars, and imaged them with adaptive optics. In 20% of systems, we detected stellar companions that were close enough to go unresolved in Kepler observations. We calculated the distribution of planet radius correction factors needed to adjust for these observed companions, along with simulations of undetected companions to which our observations were not sensitive. We then used these correction factors to optimize an occurrence rate model for small, close-in planets while correcting Kepler's detection efficiency for the presence of unresolved companions, and quantified how this correction affects occurrence estimates. Median occurrence rates for small planets between 2 and 100 days increased by an average factor of 1.08–1.19 (depending on statistical treatments), with the largest differences found for smaller planets at larger orbital periods. We found that the frequency of Earth-sized planets in the habitable zone ($\eta\oplus$) increased by a factor of $1.18^{+0.43}_{-0.66}$ $1.46^{+0.53}_{-0.83}$ when accounting for the effect of unresolved companions on Kepler's detection sensitivity.

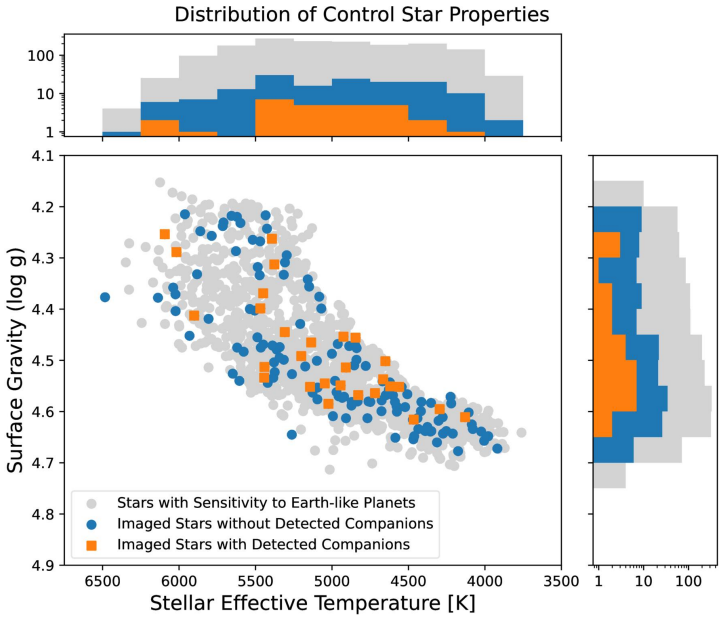

The sample of Kepler FGK dwarf stars around which a 1 $R_\oplus$ planet receiving the same insolation as Earth could have been detected. The full set of 2136 stars is shown as gray circles, using the stellar effective temperatures and (log) surface gravities available in T. A. Berger et al. (2020). The randomly selected subset of 198 Sun-like control stars we observed is shown in color: control stars with detected companions are shown as orange squares, while those without detected companions are shown as blue circles. Side panels show corresponding histograms for the (top) stellar effective temperature and (right) surface gravity distributions.

A Thick Volatile Atmosphere on the Ultrahot Super-Earth TOI-561 b

Johanna K. Teske, Nicole L. Wallack, Anjali A. A. Piette, Lisa Dang, Tim Lichtenberg, Mykhaylo Plotnykov, Raymond Pierrehumbert, Emma Postolec, Samuel Boucher, Alex McGinty, Bo Peng, Diana Valencia, and Mark Hammond

The Astrophysical Journal Letters, Volume 995, Number 2

Ultrashort-period (USP) exoplanets—with $R_p \leq 2R_\oplus$ and periods ≤1 day—are expected to be stripped of volatile atmospheres by intense host star irradiation, which is corroborated by their nominal bulk densities and previous eclipse observations, consistent with bare-rock surfaces. However, a few USP planets appear anomalously underdense relative to an Earth-like composition, suggesting an exotic interior structure (e.g., coreless) or a volatile-rich secondary atmosphere increasing their apparent radius. Here, we present the first dayside emission spectrum of the low-density (4.3 ± 0.4 g cm^{-3}) USP planet TOI-561 b, which orbits an iron-poor, alpha-rich, ~10 Gyr old thick-disk star. Our 3—5 μm JWST/NIRSpec observations demonstrate the dayside of TOI-561 b is inconsistent with a bare-rock surface at high statistical significance, suggesting instead a thick volatile envelope that is cooling the dayside to well below the ~3000 K expected in the bare-rock or thin-atmosphere case. These results reject the popular hypothesis of complete atmospheric desiccation for highly irradiated exoplanets and support predictions that planetary-scale magma oceans can retain substantial reservoirs of volatiles, opening up the geophysical study of ultrahot super-Earths through the lenses of their atmospheres.

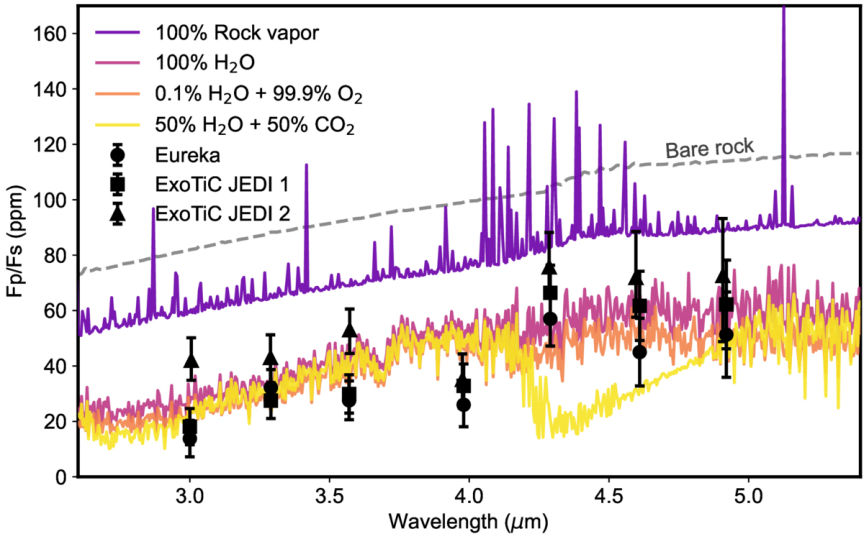

The JWST/NIRSpec emission spectrum of TOI-561 b is inconsistent with a zero-albedo bare-rock surface. The black symbols and error bars show the Eureka! (circles), ExoTiC JEDI 1 (squares), and ExoTiC JEDI 2 (triangles) reductions/fits. There is no offset appliedx between the NRS1 and NRS2 detectors (the gap around 3.75 μm). The gray dashed line shows the expected emission spectrum for a bare rocky surface assuming zero Bond albedo. The colored lines show model spectra simulated using a 1D self-consistent atmospheric model and different chemical compositions (see the legend). We assume no day–night heat redistribution in the rock vapor case and efficient day–night heat redistribution in the cases without rock vapor. Volatile-rich atmospheric compositions are able to reproduce the observed brightness temperature. The points plotted here are in Table 1.

Dust Recycling and Icy Volatile Enhancement (DRIVE): A Novel Method of Volatile Enrichment in Cold Giant Planets

Eric R. Van Clepper, Felipe Alarcón, Edwin Bergin, and Fred J. Ciesla

The Astrophysical Journal Letters, Volume 994, Number 2

Giant planet atmospheres are thought to reflect the gas phase composition of the disk when and where they formed. However, these atmospheres may also be polluted via solid accretion or ice sublimation in the disk. Here, we propose a novel mechanism for enriching the atmospheres of these giant planets with volatiles via pebble drift, fragmentation, and ice sublimation. We use a combination of 3D hydrodynamic simulations, radiative transfer, and particle tracking to follow the trajectories and resulting temperatures of solids in a disk containing an embedded planet forming outside the CO snowline. We show that small dust can become entrained in the meridional flows created by the giant planet and advected above the disk midplane where temperatures are well above the sublimation temperature of CO. This transport of small grains occurs over 10 kyr timescales, with individual micron-sized grains cycling between the midplane and surface of the disk multiple times throughout the planetary accretion stage. We find that this stirring of dust results in sublimation of CO gas above the snow surface in the dust trap created exterior to the giant planet, leading to supersolar CO abundances in the pressure bump. This mechanism of dust recycling and icy volatile enrichment in cold giant planets, which we call the DRIVE effect, may explain the enhanced metallicities of both wide-separation exoplanets and Jupiter in our own solar system.

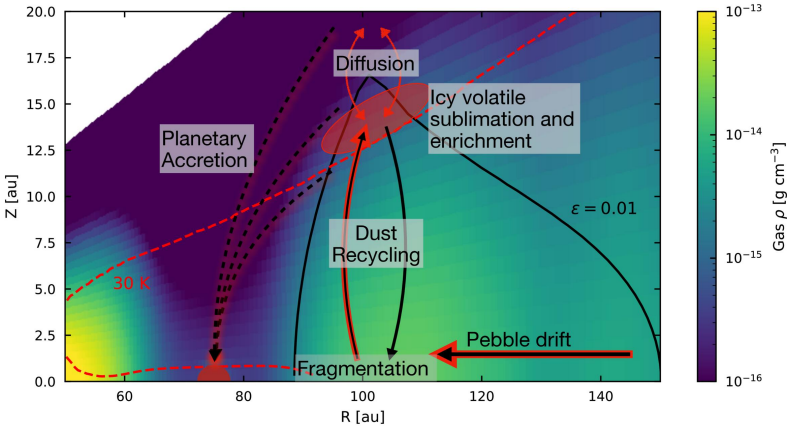

Cartoon schematic of the DRIVE effect enriching the atmosphere of a giant planet with volatiles. Larger pebbles trap volatiles from the outer disk and transport them to the pressure bump created by the giant planet via radial drift. Here, fragmentation creates fine dust, which can be lofted away from the midplane, leading to sublimation of ice mantles on the dust and enriching the gas above the snow surface with volatiles. This volatile-rich gas can then be accreted onto the planet, resulting in a volatile-enriched atmosphere. The dust, due to the lower gas density at the surface of the disk, decouples from the gas and can settle back to the midplane as a bare grain, fractionating the volatile elements from the more refractory solids. Here, the color shows the azimuthally averaged gas density from our FARGO3D simulations. The solid black contour outlines the region of the disk where the total dust-to-gas mass ratio is equal to 0.01 in our DustPy simulations, with higher dust densities below this contour. The transport of icy pebbles is represented by the black and red solid arrows, where black arrows represent bare grains and red arrows represent CO gas. Meridional flows onto the planet including entrained CO gas are illustrated by the red and black dashed arrows. The approximate location of the CO snowline at 30 K is also included.

The formation and structure of iron-dominated planetesimals

Terry-Ann Suer, Edgar S. Steenstra, Simone Marchi, John A. Tarduno, and Ilaria Pascucci

Astronomy & Astrophysics, Volume 704, Article A226

Context. Metal-rich asteroids and iron meteorites are considered core remnants of differentiated planetesimals and/or products of oxygen-depleted accretion.
Aims. Investigating the origins of iron-rich planetesimals could provide key insights into planet formation mechanisms.
Methods. Using differentiation models, we evaluate the interior structure and composition of representative-sized planetesimals (~200 km diameter), while varying oxygen fugacity and initial bulk meteoritic composition.
Results. Under the oxygen-poor conditions that likely existed early in the inner regions of the Solar System and other protoplanetary disks, core fractions remain relatively consistent across a range of bulk compositions (CI, H, EH, and CBa). Some of these cores could incorporate significant amounts of silicon (10–30 weight%) and explain the metal fractions of Fe-rich bodies in the absence of mantle stripping. Conversely, planetesimals forming under more oxidizing conditions, such as beyond snow lines, could exhibit smaller cores, enriched in carbon, sulfur (>1 wt%), and oxides. Sulfur-rich cores, like those formed from EH and H bulk compositions, could remain partly molten, sustain dynamos, and even drive sulfur-rich volcanism. Additionally, bodies with high carbon contents, such as CI compositions, can form graphitic outer layers.
Conclusions. These variations highlight the importance of initial formation conditions in shaping planetesimal structures. Future missions, such as NASA's Psyche mission, offer an opportunity to measure the relative abundances of key elements (Fe, Ni, Si, and S) necessary to distinguish among formation scenarios and structure models for Fe-rich and reduced planetesimals.

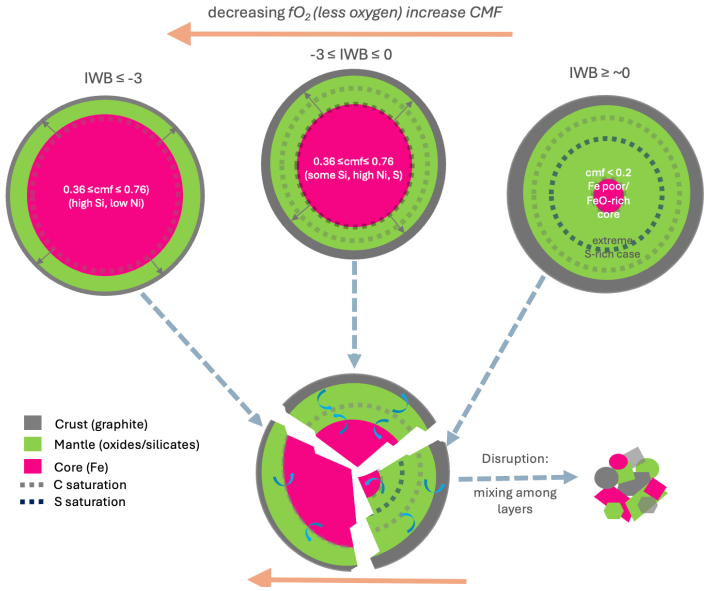

Plausible planetesimal structures resulting from a range of redox and disruption scenarios. Redox-sensitive results indicate that relatively small cores form for most bulk compositions above IW, but core sizes can change dramatically between $-3 \leq \Delta IW \leq 0$. Disruption can produce additional scenarios that are either Fe- or silicate-rich, depending on the details of the events. Mantle stripping can lead to bodies with larger CMFs as well as bodies formed from mixed fragments (Asphaug & Reufer 2014).

Detection and characterisation of a 106-day transiting Jupiter: TOI-2449 b/NGTS-36b

S. Ulmer-Moll, S. Gill, R. Brahm, A. Claringbold, M Lendl, K. Al Moulla, D. Anderson, M. Battley, D. Bayliss, A. Bonfanti, F. Bouchy, C. Briceño, E. M. Bryant, M. R. Burleigh, K. A. Collins, A. Deline, X. Dumusque, J. Eberhardt, N. Esponoza, B. Falk, J. P. Faria, J. Fernández, P. Figueira, M. Fridlund, E. Furlan, M. R. Goad, R. F. Goeke, J. Hagelberg, F. Hawthorn, R. Helled, Th. Henning, M. Hobson, S. B. Howell, M Jafariyazani, J. M. Jenkins, J. S. Jenkins, M. I. Jones, A. Jordán, A. Kendall, N. Law, C. Littlefield, A. W. Mann, J. McCormac, C. Mordasini, M. Moyano, H. Osborn, C. Pezzotti, A. Psaridi, S. N. Quinn, T. Rodel, J. E. Rodriguez, F. Rojas, S. Saha, M. Schlecker, S. Seager, S. G. Sousa, M. Tala Pinto, T. Trifonov, S. Udry, J. I. Vines, G. Vivani, C. A. Watson, P. J. Wheatley, T. G. Wilson, J. N. Winn, G. Zhou, C. Ziegler

Astronomy & Astrophysics, Volume 703, Article A258

Context. Only a handful of transiting giant exoplanets with orbital periods longer than 100 days are known. These warm exoplanets are valuable objects, as their radius and mass can be measured and lead to an in-depth characterisation of the planet's properties. Thanks to low levels of stellar irradiation and large orbital distances, the atmospheric properties and orbital parameters of warm exoplanets remain relatively unaltered by their host star, giving new insights into planetary formation and evolution. Aims. Our aim is to increase the sample of warm giant exoplanets with precise radii and masses. Our goal is to identify suitable candidates in the Transiting Exoplanet Survey Satellite data and perform follow-up observations with ground-based instruments. Methods. We used the Next Generation Transit Survey (NGTS) to detect additional transits of planetary candidates in order to pinpoint their orbital period. We also monitored the target with several high-resolution spectrographs to measure the planetary mass and eccentricity. We studied the planet's interior composition with a planetary evolution code to determine the planet's metallicity. Results. We report the discovery of a 106-day period Jupiter-sized planet around the G-type star TOI-2449/NGTS-36. We jointly modelled the photometric and radial velocity data and find that the planet has a mass of $0.70_{-0.04}^{+0.05}$ M_J and a radius of 1.001 ± 0.009 R_J. The planetary orbit has a semi-major axis of 0.449 au and is slightly eccentric (e = $0.0098_{-0.030}^{+0.028}$). We detected an additional 3-year signal in the radial velocity data that is likely due to the stellar magnetic cycle. Based on the planetary evolution models considered here, we find that TOI-2449 b/NGTS-36 b contains 11_{-5}^{+6} $M_\oplus$ of heavy elements and has a marginal planet-to-star metal enrichment of $3.3_{-1.8}^{+2.5}$. Assuming a Jupiter-like bond albedo, TOI-2449 b/NGTS-36 b has an equilibrium temperature of 400 K and is a good target for understanding nitrogen chemistry in cooler atmospheres.

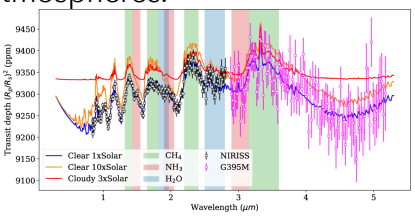

Synthetic transmission spectra of TOI-2449 b from petitRADTRANS (Mollière et al. 2019), assuming equilibrium chemistry and an isothermal atmosphere. We used 1×, 3×, and 10× models with a solar C/O ratio and include a grey cloud deck at 1 mbar for the cloudy model. Simulated flux measurements from NIRISS/SOSS and NIRSpec/G395M instrument are shown as black and pink points.

HWO Target Stars and Systems: A Prioritized Community List of Potential Stellar Targets for Habitable Worlds Observatory's ExoEarth Survey

Noah W. Tuchow, Caleb K Harada, Eric E. Mamajek, Angelle Tanner, Natalie R. Hinkel, Ruslan Belikov, Dan Sirbu, David R. Ciardi, Christopher C. Stark, Rhonda M. Morgan, Dmitry Savransky, and Michael Turmon

Publications of the Astronomical Society of the Pacific, Volume 137, Number 10

The HWO Target Stars and Systems 2025 (TSS25) list is a community-developed catalog of potential stellar targets for the Habitable Worlds Observatory (HWO) in its survey to directly image Earth-sized planets in the habitable zone. The TSS25 list categorizes potential HWO targets into priority tiers based on their likelihood to be surveyed and the necessity of obtaining observations of their stellar properties prior to the launch of the mission. This target list builds upon previous efforts to identify direct imaging targets and incorporates the results of multiple yield calculations assessing the science return of current design concepts for HWO. The TSS25 list identifies a sample of target stars that have a high probability to be observed by HWO (Tiers 1 and 2), independent of assumptions about the mission's final architecture. These stars should be the focus of community precursor science efforts in order to mitigate risks and maximize the science output of HWO. This target list is publicly available and is a living catalog that will be continually updated leading up to the mission.

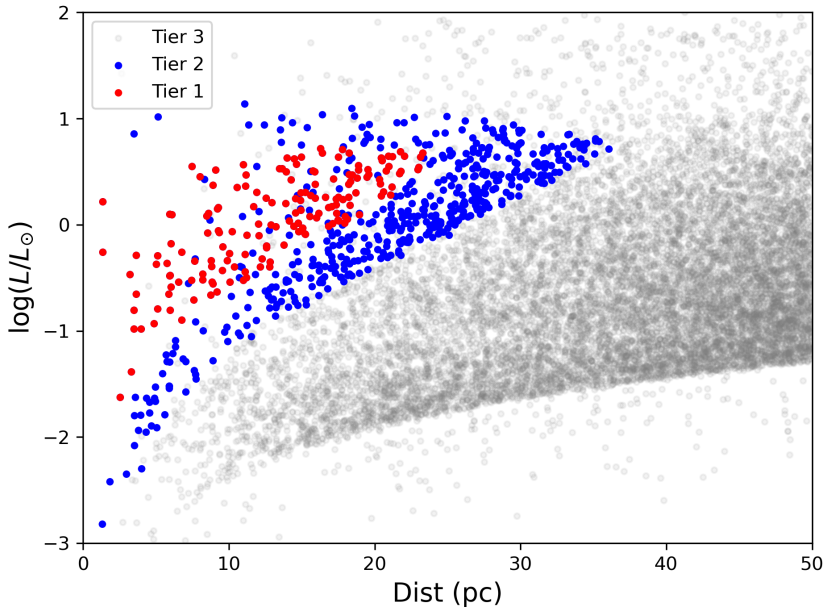

Targets in all tiers of our catalog plotted in distance vs. luminosity space, with the tiers indicated by color.

Radius valley scaling among low-mass stars with TESS

Harshitha M. Parashivamurthy, Gijs D. Mulders

Astronomy & Astrophysics, Volume 703, Number A8

The Transiting Exoplanet Survey Satellite (TESS) has been highly successful in detecting planets in close orbits around low-mass stars, particularly M dwarfs. This presents a valuable opportunity to conduct detailed population studies to understand how these planets depend on the properties of their host stars. The previously observed radius valley in Sun-like stars has also been observed among M dwarfs; however, how its properties vary when compared with more massive stars remains uncertain. We select the volume limited Bioverse stellar catalog, with precise photometric stellar parameters, which was cross-matched with the planet catalog consisting of TESS objects of interests (TOI) candidates and confirmed planets. We detect the radius valley around M dwarfs at a location of 1.64 ± 0.03 $R_\oplus$ and with a depth of approximately 45%. The radius valley among GKM stars scales with stellar mass as $R_p \propto M_*^{0.15\pm0.04}$. The slope is consistent, within 0.3σ, with those around Sun-like stars. For M dwarfs, the discrepancy is 3.6σ with the extrapolated slope from the Kepler FGK sample, marking the point where the deviation from previous results begins. Moreover, we do not see a clear shift in the radius valley between early and mid M dwarfs. The flatter scaling of the radius valley for lower-mass stars suggests that mechanisms other than atmospheric mass loss through photoevaporation may shape the radius distribution of planets around M dwarfs. A comparison of the slope with various planet formation and evolution models leads to a good match with pebble accretion models including water worlds, indicating a potentially different regime of planet formation that can be probed with exoplanets around the lowest-mass stars.

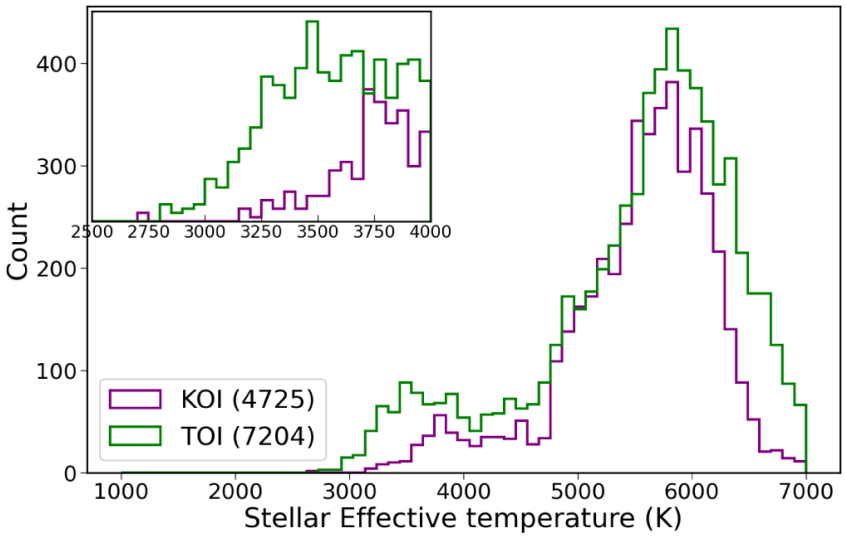

Histogram comparing TESS objects of interest (TOIs) and Kepler objects of interest (KOIs) from the NASA Exoplanet Archive, with star counts indicated in parentheses. The inset plot (top left) highlights the significant increase in low-mass stars identified by TESS, which enhances our ability to study these stars in greater detail.